Bias in the ACT DR5 SZ Cluster Catalog

Kabir Dubey
University of Chicago

December 2020

Abstract

The Sunyaev Zel'dovich (SZ) effect is a powerful and popular tool for cosmological surveys of galaxy clusters. This paper will explain how the ACT 2020 survey used the thermal SZ effect by recreating cluster distribution plots from the survey's catalog, Hilton et al 2020. By comparing the mass measurements with a Press-Schechter halo mass function, multiple indications for malmquist bias in the dataset are shown.

1 Introduction

Galaxy clusters are groups of galaxies that are bound by gravity. Ever since the Swiss astronomer Fritz Zwicky discovered dark matter within the Coma Cluster in the 1930s, galaxy clusters have served as powerful probes for cosmology. Cluster data has supported research about the accelerated expansion of the universe (Hoessel, Gunn, & Thuan 1980) and the discovery of dark energy from Type Ia supernova (SNIa) surveys. Recent studies have used cluster counts to confirm that the presence of dark energy and dark matter is much greater than baryonic material (Komatsu et al. 2011).

The background radiation from the Big Bang is known as the Cosmic Microwave Background (CMB). These photons interact with all the matter between the last scattering surface and observers. When interacting with the electrons within the hot plasma of galaxy clusters, the CMB photons undergo Inverse-Compton scattering. This means that the electrons energize

and scatter the CMB photons, creating a deficit of microwave photons in the direction of galaxy clusters; this is known as the thermal Sunyaev-Zel'dovich (tSZ) effect (Sunyaev & Zel'dovich 1970; Sunyaev & Zel'dovich 1972). The result is a decrement in microwave observations which can be used to locate clusters without knowing their redshift.

Figure 1 plots the spectral distortion of the CMB due to the tSZ effect. For 1000 evenly spaced numbers v between 1 and 800 billion, the Planck-body formula gives the change in intensity $\partial I_v = -y\frac{xe^x}{e^x-1}(4 - x\coth(\frac{x}{2}))I_v$. Take $y = 1$, $I_v(T) = \frac{2\hbar v^3}{c^2}\frac{1}{e^x-1}$, the norm frequency $x \equiv \frac{\hbar v}{k_b T_{rad}}$, and $T_{rad} = 2.7$ K (Moscardini 2009). The cluster mass can be determined by deriving the clusters' gas fraction from the tSZ effect. Assuming hydrostatic equililbrium, the amplitude of the tSZ signal is proportional to the mass of the cluster.

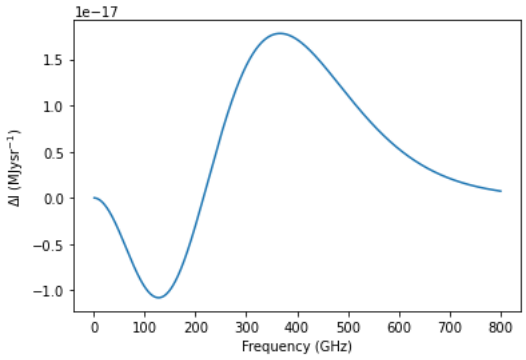

Figure 1: The spectral distortion of the CMB due to the tSZ effect.

In this paper, the Press-Schechter model is used to define a "halo mass function" that predicts galaxy halos. Derived from General Relativity, Press-Schechter theory imagines the number of objects of a certain mass within a given volume of the universe by assuming that the density field has a Gaussian distribution (Press & Schechter 1974). The Press-Schechter model relates cosmological parameters to the number of galaxy clusters within a given comoving volume. Mass data exists from galaxy clusters recorded using the tSZ effect. This paper will recreate plots of these galaxy clusters from Hilton et al. 2020 and comment on bias.

2 Data

The ACT is the Atacama Cosmology Telescope in the Parque Astronòmico Atacama in Northern Chile. The data in this paper is derived from a FITS table made publicly available at the NASA Legacy Archive for Microwave Background Data (LAMBDA) as part of the fifth ACT data release (ACT DR5). The catalog combines observations by ACT from 2008-2018 with new multi-frequency data (98 and 150 GHz). Specifically the SZ cluster search area covers $13,211$ deg2 (Hilton et al. 2020).

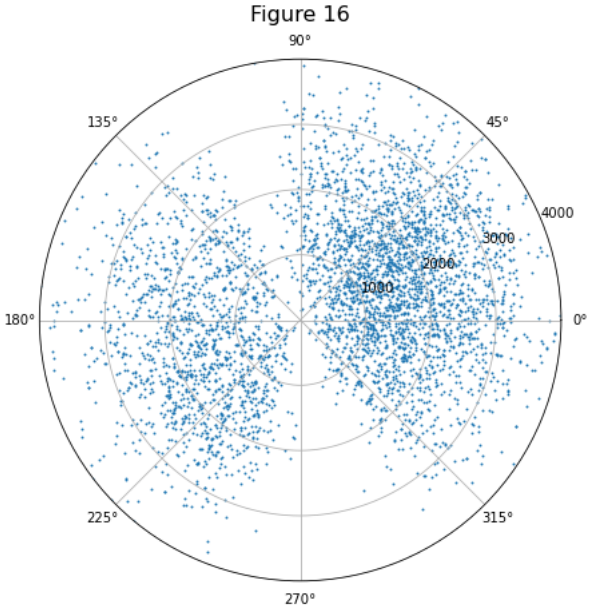

Figure 2: The left panel of figure 16 from Hilton et al 2020.

Figure 2 is a wedge plot showing the contents of the entire catalog. The angular coordinate is right ascension (RA) in degrees, increasing anticlockwise. Each point represents a galaxy cluster. The clusters are radially distributed in terms of their redshift z converted to co-moving distance coordinates in the equatorial plane. This conversion first calculates the function,

$$E(z) \equiv \sqrt{\Omega_M(1+z)^3 + \Omega_R(1+z^2) + \Omega_\Lambda} \tag{1}$$

where the density parameters $\Omega_M = 0.3$, $\Omega_R = 0.0$, and $\Omega_\Lambda = 0.7$ and then integrates,

$$D_C = D_H \int_0^z \frac{dz'}{E(z')} \tag{2}$$

where the Hubble distance $D_H \equiv 9.26 \times 10^{25} h^{-1}$m gives the co-moving distance D_C in Mpc (Hogg 1999). There are more clusters on the right of the plot than the left because the ACT surveyed more sky area at those RA coordinates (Hilton et al 2020).

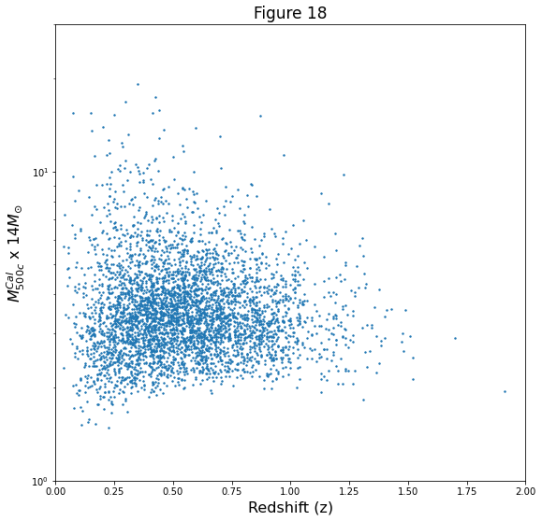

Figure 3: Figure 18 from Hilton et al 2020, but with only the ACT data.

Figure 3 is a scatterplot of the galaxy clusters in the mass-redshift plane. Notice the deficit of clusters for redshifts $1 < z < 1.1$. Figure 2 corroborates that there are regions of RA where no clusters are observed because of limits to the ACT. This may arise from bias in the photometric redshifts (Hilton et al 2020).

3 Analysis

The Press-Schechter formalism can predict the cluster distribution for the comoving volume elements in the ACT dataset. This expected distribution is compared with the measured result to better understand potential biases.

The comoving volume V_C is given by,

$$dV_C = D_H \frac{(1+z)^2 D_A^2}{E(z)} \, d\Omega dz \tag{3}$$

which is equivalent to,

$$V_C = D_H \frac{D_C(z)^2}{E(z)} \tag{4}$$

where the function $D_C(z)$ is equation 2 and $E(z)$ is equation 1 (Hogg 1999). Figure 4 indicates that the dataset reaches around 90% completeness at masses greater than 14.6 solar masses. This is used as a cutoff mass value because larger masses are more likely to experience survey bias.

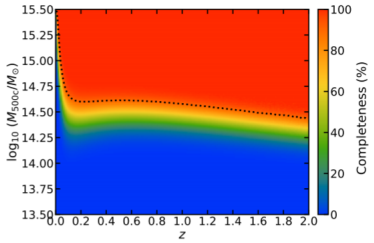

Figure 7. The completeness for $\mathrm{SNR}_{2.4} > 5$ as a function of redshift, in terms of M_{500c}^{UPP}, over the full 13,211 deg^2 survey footprint. The Tinker et al. (2008) halo mass function and Arnaud et al. (2010) scaling relation are assumed (see Section 2.4). The dashed black contour marks the 90% completeness limit.

Figure 4: Figure 7 from Hilton et al 2020.

Figure 5 plots the halo mass function. The tSZ effect can only consider relatively massive galaxy clusters, so there are fewer massive clusters to observe and the power law is strictly decreasing. But, for small masses the mass count precipitates to zero instead of reaching a maximum. Thus, there exist small mass clusters that are not luminous enough to be measured; the dataset has a malmquist bias.

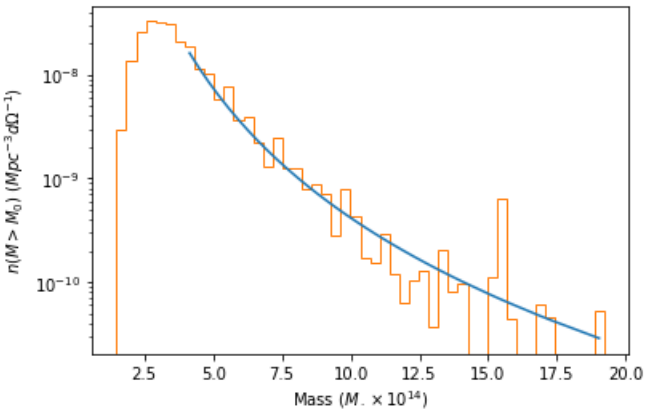

Figure 5: Comoving volume element of the halo mass function from redshift $z = 0$ to $z = 3$. Fit to a power law.

4 Discussion

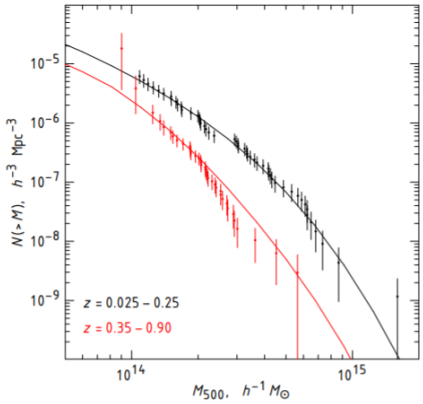

FIG. 1.— Estimated mass functions for our cluster samples computed for the $\Omega_M = 0.25$, $\Omega_\Lambda = 0.75$, $h = 0.72$ cosmology. Solid lines show the mass function models (weighted with the survey volume as a function of M and z), computed for the same cosmology with only the overall normalization, σ_8, fitted. The deficit of clusters in the distant sample near $M_{500} = 3 \times 10^{14}\ h^{-1}\ M_\odot$ is a marginal statistical fluctuation — we observe 4 clusters where 9.5 are expected, a 2σ deviation (cf. Fig. 17 in Paper II).

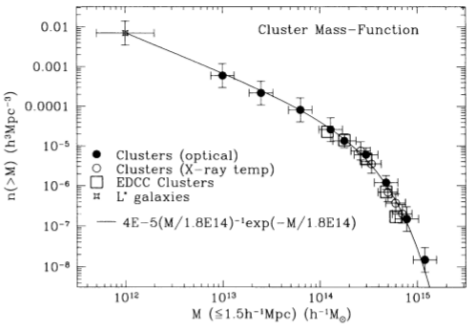

FIG. 1.—The cluster mass function as determined from optical observations (§ 2), the atomated EDCC clusters (§ 2), and the X-ray temperature function (§ 3). The L^* galaxies refer to noncluster galaxies, with typical observed mass within 0.4 h^{-1} Mpc (§ 2). The best-fit curve, $n(>M) = 4 \times 10^{-5}(M/M^*)^{-1}$ exp $(-M/M^*)$ h^3 Mpc^{-3}, with $M^* = (1.8 \pm 0.3) \times 10^{14}\ h^{-1}\ M_\odot$, is shown as the solid line.

(a) Figure 6a: Halo mass function from Vikhlinin et al 2008.

(b) Figure 6b: Halo mass function from Bahcall & Cen 1992.

Figure 6b shows the mass function from X-ray and optical observations and the Edinburgh-Durham Cluster Catalog (EDCC). Figure 6a shows a newer

mass function from two cluster samples compiled from Röntgen Satellite (ROSAT) X-ray surveys. Notice that the mass function in Figure 5 is orders of magnitude smaller than Figure 6a and 6b. The smaller overall measurements further indicates that the ACT survey is incomplete.

Malmquist bias is a core problem is cosmology. The "missing satellites problem" discusses the mismatch between observed and predicted matter distributions. The inconsistencies in the ACT survey suggest that this is because the predicted galaxies are dim, but not massless. Indeed, tSZ surveys are only sensitive to masses above a certain threshold. Once this bias is understood, it can be corrected.

There are many corrective measures for survey bias being researched. For example the signal-to-noise (SNR) manipulations in figure 4 establishes more accurate analysis that is beyond the scope of this paper. In section 2.4, Hilton et al 2020 estimates the completeness of their ACT survey using mock catalogs generated through Monte Carlo simulations. Their results substantiate that "[t]he survey is slightly more sensitive to lower mass clusters" than other surveys, which may explain the scaling issue mentioned in the beginning of this section. Hilton et al conclude that better detectors that observe for longer periods of time have a better SNR for detecting tSZ galaxy clusters.

5 Conclusions

This paper studied the SZ cluster survey catalogued in Hilton et al 2020 by recreating plots and identifying survey bias. As fields get deeper, the survey and plot completeness increases for progressively smaller masses, allowing for better overall cosmology. More sensitive CMB experiments like the CMB-S4 would yield more complete catalogs that suffer from less bias.

6 Acknowledgements

I am greatful to Joey Golec for guiding me through this project. I also thank the University of Chicago Society of Physics Students and the University of Chicago Physics department for the opportunity.

7 References

Bosch, Frank Van Den, Astro610-lecture9.pdf. (Fall 2020). Retrieved January 6, 2021, from http://www.astro.yale.edu/vdbosch/astro610-lecture9.pdf

Carlstrom, J. E., Holder, G. P., & Reese, E. D. (2002). Cosmology with the Sunyaev-Zel'dovich Effect. Annual Review of Astronomy and Astrophysics, 40(1), 643–680.
https://doi.org/10.1146/annurev.astro.40.060401.093803

Hilton, M., Sifón, C., Naess, S., Madhavacheril, M., Oguri, M., Rozo, E., Rykoff, E., Abbott, T. M. C., Adhikari, S., Aguena, M., Aiola, S., Allam, S., Amodeo, S., Amon, A., Annis, J., Ansarinejad, B., Aros-Bunster, C., Austermann, J. E., Avila, S., ... Zhang, Y. (2020). The Atacama Cosmology Telescope: A Catalog of ¿ 4000 Sunyaev-Zel'dovich Galaxy Clusters. ArXiv:2009.11043 [Astro-Ph]. http://arxiv.org/abs/2009.11043

Hoessel JG, Gunn JE, Thuan TX. 1980. ApJ 241:486–492

Hogg, D. W. (1999). Distance measures in cosmology. 15.
https://arxiv.org/abs/astro-ph/9905116

Komatsu E, Smith KM, Dunkley J, Bennett CL, Gold B, et al. 2011. ApJS 192:18

Moscardini, Laura, The Sunyaev-Zel'dovich (SZ) effect(s), (May 2009). Retrieved June 13, 2021

Neta A. Bahcall, & Chen, R. (1993). THE MASS FUNCTION OF CLUSTERS OF GALAXIES. American Astronomical Society.

Press, William H. and Schecter, Paul. (1974). "Formation of Galaxies and Clusters of Galaxies by Self-Similar Gravitational Condensation," Apj. https://ui.adsabs.harvard.edu/abs/1974ApJ...187..425P

Sunyaev, R.A., Zeldovich, Y.B. Small-scale fluctuations of relic radiation. Astrophys Space Sci 7, 3–19 (1970). https://doi.org/10.1007/BF00653471

Sunyaev, R. A., & Zeldovich, Ya. B. 1972, Comments Astrophys. Space Phys., 4, 173

Vikhlinin, A., Kravtsov, A. V., Burenin, R. A., Ebeling, H., Forman, W. R., Hornstrup, A., Jones, C., Murray, S. S., Nagai, D., Quintana, H., & Voevodkin, A. (2009). Chandra Cluster Cosmology Project III: Cosmological Parameter Constraints. The Astrophysical Journal, 692(2), 1060–1074. https://doi.org/10.1088/0004-637X/692/2/1060

Weinberg, David H. A162, Lecture 26 Dark Matter. (February 1997). Retrieved January 6, 2021,
from http://www.astronomy.ohio-state.edu/ dhw/Intro/lec26.html